

---

# FTerViT: Fully Ternary Vision Transformer

---

Szymon Ruciński<sup>1,2</sup> Pietro Bonazzi<sup>2</sup>

szymon.rucinski@csem.ch pbonazzi@ethz.ch

Engin Türetken<sup>1</sup> Simon Narduzzi<sup>1</sup> Michele Magno<sup>2</sup> Nadim Maamari<sup>1</sup>

<sup>1</sup>CSEM, Neuchâtel, Switzerland <sup>2</sup>ETH Zürich, Zurich, Switzerland

## Abstract

Ternary Vision Transformers offer substantial model compression, however state-of-the-art methods only ternarize the encoder layers, leaving patch embeddings, LayerNorm parameters, and classifier heads in full precision. In compact models targeting resource-constrained processors, such as microcontrollers, these remaining full-precision components determine the total memory footprint, severely limiting deployment efficiency and on-device feasibility. In this work, we introduce a fully ternarized Vision Transformer in which *all* weight matrices and normalization parameters are ternarized (FTerViT). To this end, we introduce two novel operators : TernaryBitConv2d with per-channel scaling for patch embedding and TernaryLayerNorm. FTerViT is trained using knowledge distillation, followed by a lightweight quantization-aware recovery phase. Our ternary W2A8 DeiT-III-S at  $384 \times 384$  resolution achieves 82.43% ImageNet-1K top-1 at 6.09 MB ( $\sim 15 \times$  compression,  $-2.42$  pp vs. FP32), outperforming prior ternary ViTs methods up to 8 pp. Finally, we demonstrate the first implementation of ternary vision transformers on a dual cores XTensa LX7 microcontroller inside the ESP32-S3 system-on-chip. By deploying FTerViT-Small (based on DeiT-III-Small at  $224 \times 224$  resolution, 5.81 MB), we achieve 79.64% ImageNet-1K top-1 accuracy.

## 1 Introduction

Vision Transformers (ViTs) [1, 2, 3] are strong image classifiers, yet their substantial memory footprint makes them poorly suited for microcontroller-class devices. A standard compact ViT like DeiT-Small [3] requires 88.3 MB in FP32, while typical microcontroller units (MCUs) offer only a few megabytes of external RAM. This mismatch is particularly problematic for always-on, low-power vision applications where cloud offloading is undesirable or infeasible [4].

Ternary quantization offers a compelling solution [5, 6]. By constraining the weights to  $\{-1, 0, +1\}$  and packing them in 2 bits, ternary models can theoretically achieve  $16 \times$  weight compression relative to FP32 models. However, existing low-bit ViTs [6, 5, 7, 8, 9, 10, 11, 12, 13, 14], only ternarize the encoder layers, leaving the patch embedding, LayerNorm, and classifier head at INT8 or FP32. While at moderate bitwidths, these exceptions are tolerable; at 2-bits, they become the dominant bottleneck. In DeiT-Tiny [2], the non-ternary components account for less than 4% of parameters yet consume 38% of the model size (Fig. 1b). Our proposed method ternarizes the patch embedding, LayerNorm, and classifier head jointly (Table 3).

This design choice stems from well-known sensitivity of quantizing the first and last layers [15, 13, 14, 10, 11] predating the invention of ViTs [16, 17, 18]. Recently, TerViT [6], reports significant accuracy drops (22.4 pp) for full-ternarization of the patch embedding and final classifier. In TerViT, LayerNorm parameters are similarly left un-quantized due to activation outliers and inter-channel variation [19, 20, 21, 22, 23, 24, 25]. DeiT-Small [2] showcases its patch embedding as the single most sensitive layer ( $4.7 \pm 0.5\%$  of total importance, Section 3.1) under a Taylor first-order analysis [26].

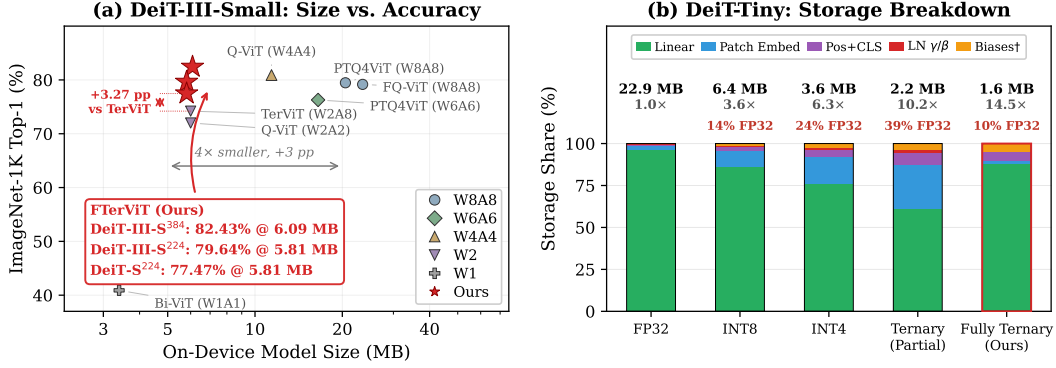


Figure 1: **(a)** DeiT-III-Small size vs. accuracy; FTerViT (W2A8): 82.43% at 6.09 MB ( $384^2$ ) / 79.64% at 5.81 MB ( $224^2$ ). FTerViT based on DeiT-S<sup>224</sup> reaches 77.47% under ternary quantization. **(b)** DeiT-Tiny storage; partial-W2 leaves 38% of bytes at FP32, fully ternary drops the share to 10%. DeiT-III-Small follows the same trend (24% partial, 4% fully ternary; 88.3 MB  $\rightarrow$  5.81 MB).

The resulting model substantially narrows the gap between standard ViT accuracy and MCU-scale deployment constraints. FTerViT-Small based on DeiT-III-S<sup>224</sup> occupies 5.81 MB and reaches 79.64% ImageNet-1K top-1. Based on DeiT-III-S<sup>384</sup>, it reaches 82.43% at 6.09 MB, losing 2.42 pp from FP32 and reducing the TerViT-DeiT-S accuracy gap from 5.7 pp to 2.4 pp (Fig. 1a). The  $224 \times 224$  model runs on a \$10 ESP32-S3 with 8 MB PSRAM, while the original 88.3 MB FP32 model remains far beyond the device memory budget.

The main contributions of the paper are summarized as follows:

- We are the first to show that the most fragile components of ViT: patch embedding, LayerNorms, and classifier head can be ternarized to  $\{-1, 0, +1\}$  when trained with knowledge distillation. Our work pushes the boundary of what was considered quantizable.
- Our approach maintains strong accuracy at extreme compression: 82.43% top-1 on ImageNet-1K at 6.09 MB (14.6 $\times$  compression), losing 2.42 pp from FP32. Our FTerViT-DeiT-S achieves 3.27 pp higher ImageNet-1K top-1 than TerViT-DeiT-S [6].
- We propose a simple yet effective training strategy based on same-architecture knowledge distillation and lightweight recovery fine-tuning, enabling substantially faster convergence and improved final accuracy over prior ternary ViT training approaches.
- We demonstrate a standalone C implementation of a ternary Vision Transformer on the dual-core ESP32-S3, a resource-constrained commodity MCU platform with only 8MB of memory. We validate the practical feasibility of fully ternary ViTs for resource-constrained edge devices.

## 2 Methodology

FTerViT is designed to enable fully ternary Vision Transformers retaining competitive accuracy while satisfying the strict memory constraints (below 10MB) of microcontroller-class hardware. Achieving this goal is challenging because several components beyond the transformer encoder – most notably patch embeddings and normalization layers – are highly sensitive to quantization and are therefore typically retained in FP32 by prior work.

This section presents the FTerViT, which is a full ternary adaptation of DeiT-Tiny [2] (5.5M params, 22.9 MB FP32) and DeiT-Small [3] (22.1M params, 88.3/88.9 MB FP32 at  $224/384$  resolution) trained on ImageNet-1K. The main design of FTerViT is structured around two core elements: (1) a complete set of ternary primitives (Section 2.1) and (2) a two-phase knowledge distillation procedure that enables stable quantization (Section 2.2).

### 2.1 Ternary Primitives: TernaryBitLinear, TernaryBitConv2d, TernaryLayerNorm

We replace the three types of weight-carrying components in a ViT with dedicated ternary modules: TernaryBitLinear for fully-connected layers, TernaryBitConv2d for the patch-embedding convolution,

and TernaryLayerNorm for LayerNorm affines. Together, these operators eliminate all remaining FP32 bottlenecks while maintaining compatibility with standard ViT architectures.

**TernaryBitLinear:** As defined in BitNet-1.58b [27], TernaryBitLinear quantizes weights to  $\{-1, 0, +1\}$  and activations to 8-bit integers. For a weight matrix  $\mathbf{W} \in \mathbb{R}^{n \times m}$ , the ternary quantization is:

$$\tilde{\mathbf{W}} = s_w \cdot \text{RoundClip}\left(\frac{\mathbf{W}}{s_w + \epsilon}, -1, +1\right), \quad (1)$$

where the clamped rounding operator is:

$$\text{RoundClip}(x, a, b) = \max(a, \min(b, \text{round}(x))), \quad (2)$$

and  $s_w$  is the per-tensor *absmean* (mean absolute value) of the weight matrix:

$$s_w = \text{absmean}(\mathbf{W}) = \frac{1}{nm} \sum_{i,j} |\mathbf{W}_{ij}|. \quad (3)$$

Absmean is preferred over max-based scaling because  $\max |W|$  obviously pushes most ratios  $|W|/s_w \ll 1$  into the zero bin of the ternarized grid. Consistent with this intuition, TWN [28] similarly derives the optimal threshold  $\Delta^* \approx 0.75 \mathbb{E}|W|$  analytically for Gaussian weights, well below  $\max |W|$ .

Following BitNet b1.58 [27], we RMS-normalize and quantize input activations of a layer to 8-bit integers via per-token absmax scaling,

$$s_x = \frac{127}{\max_i |x_i|}, \quad \tilde{x} = \text{RoundClip}(s_x x, -128, 127) / s_x. \quad (4)$$

Gradients pass through both quantization operations via the straight-through estimator (STE) [29].

**TernaryBitConv2d:** For the patch embedding layer, we introduce TernaryBitConv2d, which applies per-channel scaling to better handle heterogeneous filter magnitudes [30, 31]. For an activation map  $x^{(c)} \in \mathbb{R}^{H \times W}$ , let  $\Omega = \{1, \dots, H\} \times \{1, \dots, W\}$  denote its spatial grid. Each channel  $c$  has its own scales:

$$s_w^{(c)} = \frac{1}{K} \sum_k |\mathbf{W}_{\text{conv}}^{(c)}[k]|, \quad s_x^{(c)} = \frac{127}{\max_{(h,w) \in \Omega} |x^{(c)}[h,w]|}, \quad (5)$$

where  $K$  is the number of kernel elements, and  $H, W$  denote spatial size. The activation scale uses one scalar per sample and channel.

**TernaryLayerNorm:** For LayerNorm layers, we ternarize the learnable affine parameters  $\gamma$  (scale) and  $\beta$  (shift):

$$\text{TernaryLN}(\mathbf{x}) = \tilde{\gamma} \odot \frac{\mathbf{x} - \mu}{\sqrt{\sigma^2 + \epsilon}} + \tilde{\beta}, \quad (6)$$

where  $\tilde{\gamma}$  and  $\tilde{\beta}$  use the same absmean scheme as weights (3). Per-token statistics  $(\mu, \sigma^2)$ , as well as biases, are kept at FP32 since their parameter count is negligible and ternarizing them would destroy positional information. The 25 LayerNorms hold  $<0.2\%$  of parameters but account for 34–39% of Taylor-FO importance and 21–28% of Hessian-trace importance (Section 3.1).

## 2.2 Training Protocol

Our ternary student is initialized directly from the pretrained FP32 teacher and trained via quantization-aware distillation (QAD). Training proceeds in two phases. The first phase runs at learning rate (LR)  $1e-4$  with cosine decay until validation top-1 saturates (reaching 76.78% on DeiT-III-S<sup>224</sup>). During the second phase, we restart LR at  $1e-5$  with cosine decay over 10 epochs at the same loss (see Table 1). The reduction in LR enables recalibration and recovery of the final scale from Phase 1 saturation, lifting top-1 by 3–4 pp across distillation settings (Table 5).

During both steps, FTerVit is trained using forward-KL distillation [32], to match its pretrained frozen full-precision ViT equivalent [9]. Given student logits  $z_S$  and teacher logits  $z_T$ , the FTerVit loss can be simply described as:

$$\mathcal{L}_{\text{KL}} = \text{KL}(\text{softmax}(z_T) \parallel \text{softmax}(z_S)), \quad (7)$$

Prior ternary and low-bit ViTs adopt a single-phase loss, ranging from label-only cross-entropy (CE) without distillation [6, 5], attention or query/key similarity matching [13, 33], soft-logit distillation [11, 14], hard-label distillation [12], multi-step knowledge-distillation (KD) across bit-precisions [34], to combined CE+KL+feature objectives [7].

In contrast, we use only the KL term since a cross-entropy term conflicts with KL in low-bit networks [35, 36, 37]. In our experiments, we set the distillation temperature to  $T=1$  [38, 39, 40].

Table 1: Two-phase training hyperparameters. Both phases minimize only the KL loss; only the cosine learning-rate schedule changes.

	Phase 1 (Training)	Phase 2 (Fine-tuning)
Loss	$\mathcal{L}_{\text{KL}} (T=1)$	$\mathcal{L}_{\text{KL}} (T=1)$
Learning rate (cosine decay)	$1e-4$ (250 ep)	$1e-5$ (10 ep)
Optimizer	AdamW [41]	AdamW [41]
Weight decay	0.05	0.01
Batch	1024	512
Teacher	Pretrained FP32 (frozen)	Pretrained FP32 (frozen)
Student init	Ternarized from teacher	Phase 1 checkpoint

### 3 Experiments

#### 3.1 Layer Sensitivity Analysis

A core obstacle to full ternarization of Vision Transformers has been the well-documented sensitivity of the patch embedding and LayerNorm layers [6, 15, 13]. Prior work therefore retained these components in higher precision.

To quantify this sensitivity, we measure per-component importance on ImageNet-1K using two established estimators: Taylor first-order (FO) importance [26] and Hessian-trace approximation (HAWQ-style [18]).

Table 2: Per-component importance share on ImageNet-1K (mean  $\pm$  SEM). LayerNorm and patch embedding together dominate importance despite negligible parameter counts, explaining why prior ternary ViTs left them in higher precision. “Top quantizable layer” excludes non-ternarized positional/class embeddings.

Component	DeiT-Tiny (5.7M)			DeiT-Small (22.1M)		
	Params (%)	Taylor-FO (%)	Hess. (%)	Params (%)	Taylor-FO (%)	Hess. (%)
LayerNorm	0.17	<b>39.4 <math>\pm</math> 1.2</b>	<b>28.0 <math>\pm</math> 0.1</b>	0.09	<b>34.1 <math>\pm</math> 1.0</b>	<b>20.7 <math>\pm</math> 0.4</b>
FFN (FC1, FC2)	62.1	33.2 $\pm$ 0.9	28.7 $\pm$ 0.2	64.3	<b>25.9 <math>\pm</math> 0.6</b>	30.2 $\pm$ 0.7
Attention (Q, K, V, Proj)	31.1	18.4 $\pm$ 0.4	15.0 $\pm$ 0.1	32.2	17.4 $\pm$ 0.3	19.3 $\pm$ 0.2
LayerScale		—		0.04	15.7 $\pm$ 1.2	9.4 $\pm$ 0.7
Patch embed	2.6	<b>3.3 <math>\pm</math> 0.1</b>	<b>4.4 <math>\pm</math> 0.1</b>	1.3	<b>4.6 <math>\pm</math> 0.4</b>	<b>8.6 <math>\pm</math> 0.7</b>
Classifier head	3.4	1.3 $\pm$ 0.1	0.2 $\pm$ 0.0	1.7	0.3 $\pm$ 0.0	0.01 $\pm$ 0.00

**⚡ Sorted by Taylor-FO importance (descending) on DeiT-Small**

As shown in Table 2, All LayerNorms combined account for 21–39% of total importance while occupying  $<0.2\%$  of parameters. Furthermore, among all individual layers in DeiT-Small, patch embedding is the single most important one under both metrics. These findings directly explain the 22.4 pp accuracy drop reported by TerViT when attempting full ternarization [6].

### 3.2 Benchmark Results

We first compare FTerViT against prior quantized ViTs on ImageNet-1K. As shown in Table 3, FTerViT achieves the best reported accuracy among ternary DeiT-S models, reaching **77.47%** top-1 with 2-bit weights and 8-bit activations. Unlike the methods we compare against, FTerViT applies ternary quantization not only to the transformer blocks but also to the patch embedding, normalization layers, and classifier head, resulting in a fully ternary model that achieves both the best reported accuracy and the highest compression among ternary DeiT-S models. Starting from the stronger DeiT-III-S backbone further improves performance: the  $224 \times 224$  variant reaches **79.64%** top-1 ( $-3.44$  pp from its FP32 teacher), while the  $384 \times 384$  variant achieves **82.43%** top-1 ( $-2.42$  pp).

Table 3: Comparison of quantized ViT methods on ImageNet-1K (Top-1). W/A = weight/activation bits. FTerViT is *fully* ternary.

Method	W	A	Model	Size (MB)	Comp.	Regime	Epochs	Top-1
Bi-ViT [10]	1	1	DeiT-S	3.4	26×	QAT	300	40.9
BiViT [9]	1	mixed	Swin-S	15.4	13×	QAT	300	75.6
PTQ4ViT [20]	8	8	DeiT-S	22	4×	PTQ	32 imgs	79.47
RepQ-ViT [22]	6	6	DeiT-S	16.7	5.3×	PTQ	32 imgs	78.90
RepQ-ViT [22]	4	4	DeiT-S	11	8×	PTQ	32 imgs	69.03
Q-ViT [13]	2	2	DeiT-S	6.0	14.7×	QAT	300	72.1
LSQ [42, 13]	2	2	DeiT-S	6.0	14.7×	QAT	300	68.0
OFQ [14]	4	4	DeiT-S	11.4	7.7×	QAT	325	81.10
<b>TernaryViT</b>								
ViT-1.58b [5]	2	8	ViT-L	57	20×	Scratch	500+	74.25
TerViT [6]	2	8	DeiT-S	6.0	14.7×	QAT+PT	300*	74.2
<b>FTerViT (Ours)</b>	2	8	DeiT-S	<b>5.81</b>	<b>15.2×</b>	QAD	<b>260</b>	<b>77.47</b>
<b>FTerViT (Ours)</b>	2	8	DeiT-III-S <sup>224</sup>	<b>5.81</b>	<b>15.2×</b>	QAD	<b>260</b>	<b>79.64</b>
<b>FTerViT (Ours)</b>	2	8	DeiT-III-S <sup>384</sup>	<b>6.09</b>	<b>14.6×</b>	QAD	<b>260</b>	<b>82.43</b>

FTerViT uses DeiT-III-S<sup>224/384</sup> [3], whose FP32 baseline (83.08–84.85%) is higher than the DeiT-S baseline (79.86%). Furthermore, our method generalizes well to other image classification benchmarks. As reported in Appendix A.1, our DeiT-Tiny achieves 97.43% and 86.01% top-1 accuracy on CIFAR-10 and CIFAR-100, respectively. These numbers are nearly on par with the full-precision DeiT-Tiny (97.52% / 86.54%) while using only 1.53 MB of storage, equivalent to 15× reduction in model size.

**Two-Phase Training Effectiveness.** To analyze the contribution of the proposed training strategy, we study Phase 1 (high learning rate training) and Phase 2 (low learning rate recovery). As shown in Table 4, while Phase 1 converges slowly toward a stable accuracy, Phase 2 achieves substantial recovery within only a few epochs.

Table 4: FTerViT results across datasets and input resolutions. Phase 1 (250 epochs) denotes saturation performance; Phase 2 (+10 epochs) denotes final fine-tuned results.

Model	Dataset	Input Resolution	FP32	Phase 1	Phase 2
DeiT-Tiny	CIFAR-10	224 × 224	97.52%	97.43%	<b>97.43%</b>
DeiT-Tiny	CIFAR-100	224 × 224	86.54%	84.42%	<b>86.01%</b>
DeiT-Tiny	ImageNet-1K	224 × 224	72.19%	59.54%	<b>63.00%</b>
DeiT-Small	ImageNet-1K	224 × 224	79.86%	75.05%	<b>77.47%</b>
DeiT-III-Small	ImageNet-1K	224 × 224	83.08%	76.78%	<b>79.64%</b>
DeiT-III-Small	ImageNet-1K	384 × 384	84.85%	78.63%	<b>82.43%</b>

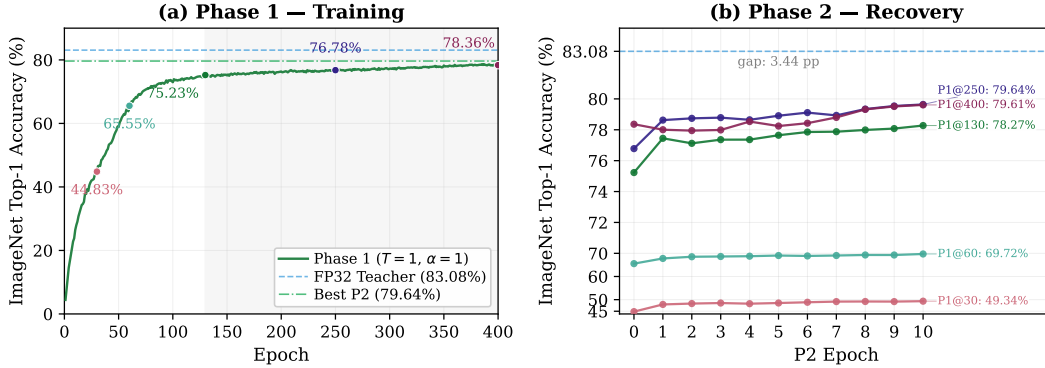


Figure 2: **(a)** Phase 1 training of DeiT-III-S<sup>224</sup> on ImageNet-1K for 250 epochs. Validation top-1 saturates near 78% and never bridges the gap to FP32 (83.08%). **(b)** Phase 2 fine-tuning from five P1 checkpoints (epochs 30–400). P1@250 converges to  $\sim$ 79.64% top-1 ( $-3.44$  pp vs. FP32) in 10 epochs. P1@400 reaches 79.61%, while early checkpoints (P1@30, P1@60) recover far less.

To better understand the source of performance gains in FTerViT, we analyze the optimization trajectory across both training phases on ImageNet-1K (DeiT-III-S<sup>224</sup>). The key finding is that Phase 2 fine-tuning is more efficient than prolonging Phase 1: a 10-epoch low-LR restart from epoch 250 outperforms 150 additional Phase 1 epochs followed by the same restart as shown in Fig. 2. More specifically, we observe the following dynamics.

**Phase 1: Saturation.** Phase 1 converges to 76–78% top-1 under cosine decay. Accuracy gains slow past epoch 130, and extending training to epoch 400 improves the Phase 1 checkpoint by only 1.6 pp (76.78%  $\rightarrow$  78.36%).

**Phase 2: Rapid Recovery.** A low-LR restart recovers accuracy within 10 epochs regardless of Phase 1 maturity as shown in Table 5. Crucially, starting Phase 2 from epoch 250 (76.78%) reaches **79.64%**, marginally higher than starting from epoch 400 (79.61%), demonstrating that the 150 extra Phase 1 epochs yield no net benefit. We finetune five P1 checkpoints (epochs 30, 60, 130, 250, 400) to confirm this pattern.

Table 5: Phase 2 finetuning trajectory from five Phase 1 checkpoints (DeiT-III-S<sup>224</sup>, ImageNet-1K). Same P2 recipe, LR cosine  $1e-5 \rightarrow 1e-6$  over 10 epochs.

P2 Ep	LR	P1@30	P1@60	P1@130	P1@250	P1@400
0	—	44.83	65.55	75.23	76.78	<b>78.36</b>
1	9.78e-6	47.93	67.79	77.45	<b>78.63</b>	78.00
3	8.15e-6	48.54	68.63	77.36	<b>78.79</b>	77.99
5	5.50e-6	48.55	69.05	77.65	<b>78.91</b>	78.24
10	1.00e-6	49.34	69.72	78.27	<b>79.64</b>	79.61

### 3.3 Component-Level Fidelity of Ternarization

We provide a detailed breakdown of ternarization effects in Fig. 3. First, ternary weights are balanced across  $\{-1, 0, +1\}$ , with 37.3% zeros (8.18 M weights), inducing sparsity that directly reduces multiply-accumulate operations at inference time. This distribution is consistent across TernaryBitLinear and classifier layers, while the patch embedding exhibits a slightly reduced zero fraction. At the representation level, patch embedding features remain closely aligned with FP32, with mean cosine similarity 0.88 (std 0.05, 5th/95th percentile 0.79/0.95), indicating stable spatial feature extraction.

Ternarization simplifies normalization: TernaryLayerNorm scale parameters converge to +1, effectively reducing normalization to identity scaling while still closely matching FP32 ( $0.979 \pm 0.007$ ).

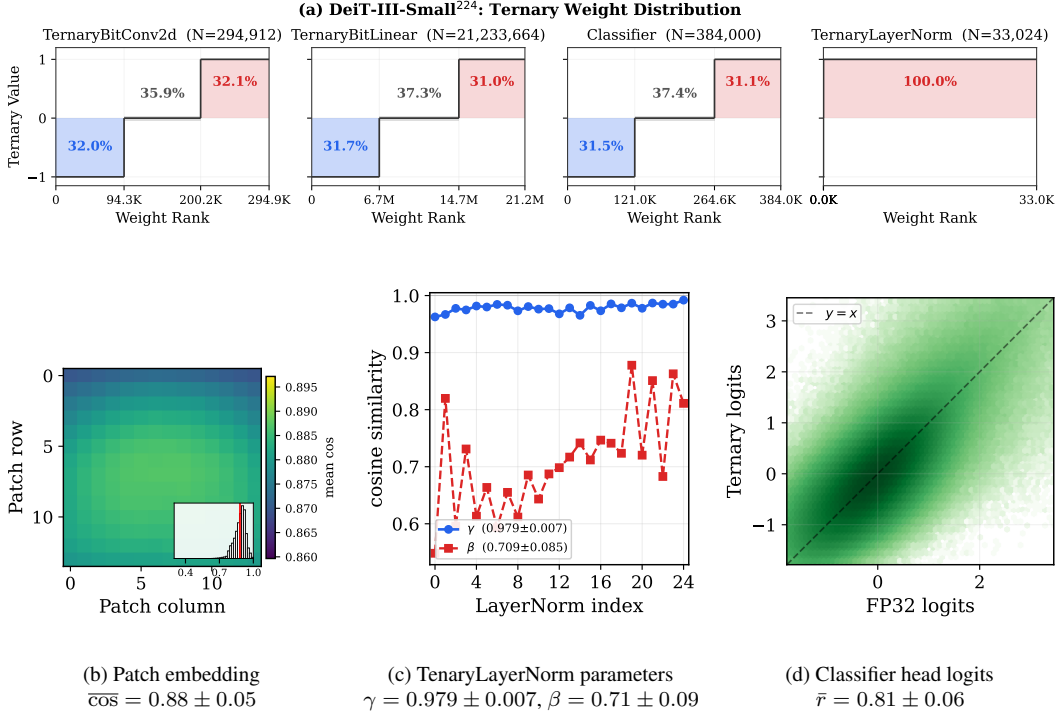


Figure 3: **Component-wise fidelity of fully ternary ViTs.** (a) Global distribution of weights constrained to  $\{-1, 0, +1\}$ . (b,c,d) FP32–ternary alignment across key components of DeiT-III-S<sup>224</sup> shows strong preservation of representational structure despite ternary quantization.

cosine). The shift parameter is reproduced less precisely ( $0.71 \pm 0.09$ ), suggesting that scale dominates.

Finally, output behavior remains consistent: classifier logits achieve mean Pearson correlation  $r = 0.81$  (std 0.06; pooled  $r = 0.79, p < 10^{-300}$ ), indicating that class rankings are largely preserved despite quantization.

### 3.4 CLS token Analysis

To gain deeper insights into the effectiveness of knowledge distillation for low-bit ternary models, we examine how the ternary student’s internal attention patterns (FTerViT-DeiT-III-S<sup>224</sup>) and component representations align with those of the full-precision (FP32) teacher. Attention rollout maps [43] computed from the final CLS token provide a principled way to visualize where each model directs its focus across the image. As shown in Figure 4, the ternary student consistently attends to the same salient semantic regions as the FP32 teacher across a diverse set of ImageNet-1K classes, indicating successful transfer of high-level visual understanding despite aggressive quantization.

## 4 On-Device Deployment and Profiling

We deploy the FTerViT based on DeiT-III-S<sup>224</sup> on a dual-core 32-bit LX7 microprocessor named ESP32-S3-EYE, shown in Fig. 5, running at 240 MHz. Our ternary model occupies 2.83 MB PSRAM at peak (FP32 activations and input image) and 5.81 MB flash (2-bit packed weights), leaving  $\sim 4.5$  MB PSRAM free on-device for camera and LCD buffers. In addition, we implement a standalone pure-C inference engine that executes all ternary layers without external dependencies. Ternary weights are bit-packed (4 weights per byte) into a 5.81 MB binary, and kernels perform integer multiply-accumulate with fused QKV projections.

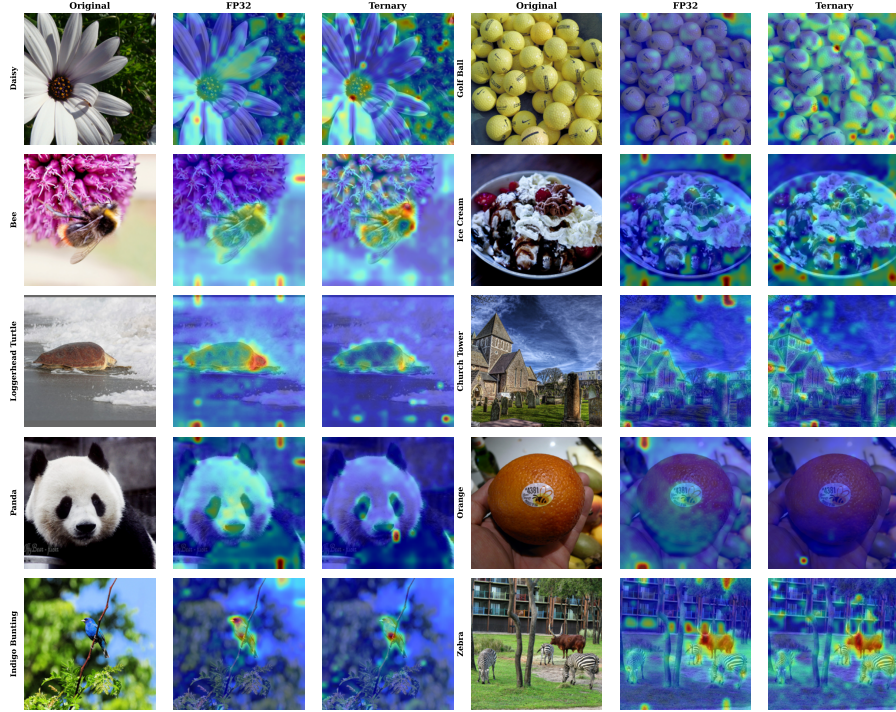


Figure 4: Attention rollout on 10 additional ImageNet-1K classes. FTerViT-DeiT-III-S<sup>224</sup> consistently attends to the same semantic regions as the FP32 teacher across diverse object categories.

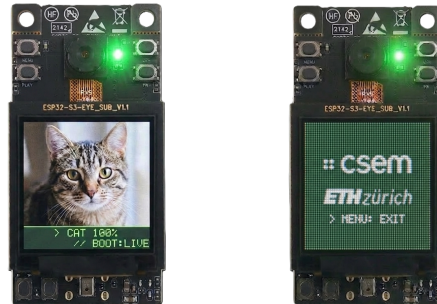


Figure 5: ESP32-S3-EYE board running on-device DeiT-III-S<sup>224</sup> ternary inference (\$10, dual-core Xtensa LX7 at 240 MHz, 8 MB PSRAM, 2 MP camera, 240×240 LCD). The 5.81 MB ternary model fits in flash (79% partition utilisation); the original 88.3 MB FP32 checkpoint is 15.2× larger and cannot load.

Our ternary model can be deployed and executed entirely on-device. A forward pass takes 21.06 s, with attention ( $Q@K^T + \text{softmax} + V$ ) and FFN each accounting for  $\approx 31\%$  of runtime, and fused QKV projections contributing a further 8.3% (see Table 7 in Appendix Section B.1).

**Power measurements.** We measure power on the ESP32-S3-EYE VOUT rail with a Nordic PPK2 probe (Fig. 6). On DeiT-Tiny FC1 (192→768), packed ternary is **1.71× faster** than FP32 (804 ms vs. 1376 ms). Subtracting board idle (149 mW), above-idle energy drops **55%** (59 mJ vs. 130 mJ). Two effects compound: 4× smaller weight storage reduces memory-bandwidth pressure, explaining the lower latency; reduced data movement lowers active power (222 mW vs. 244 mW, −9%). Active-compute power falls **22.6%** (94.8 mW → 73.4 mW).

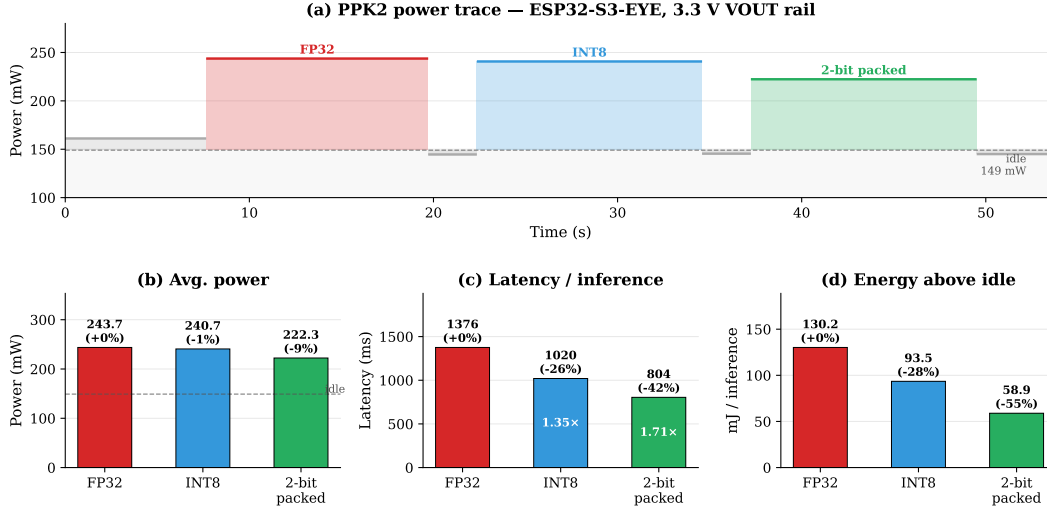


Figure 6: PPK2 power measurements on ESP32-S3-EYE (Nordic PPK2 probe, VOUT rail). **Top:** raw power trace across FP32, INT8, and 2-bit packed inference phases; dashed line = board idle (149 mW). **Bottom:** per-format power, latency, and above-idle energy per inference. Packed ternary is 1.71× faster and uses 54.7% less above-idle energy than FP32.

**Comparison with prior MCU implementation of ViT.** Prior MCU-scale Vision Transformers typically rely on neural architecture search combined with INT8 quantization to meet memory constraints. For example, MCUFormer [44] achieves 73.62% on ImageNet-1K at 0.90 MB, TinyFormer [45] reaches 96.10% on CIFAR-10 at 0.91 MB, and LMaNet-Elite [46] reports 74.50% on CIFAR-100 under 1 MB. In contrast, FTerViT follows an orthogonal approach: instead of redesigning the architecture, we compress DeiT-III-S<sup>224</sup> from 88.3 MB to 5.83 MB via ternarization, achieving 79.64% on ImageNet-1K (+5.14 pp over MCUFormer).

## 5 Conclusion

FTerViT shows that all weight matrices and normalization parameters in a ViT can be constrained to  $\{-1, 0, +1\}$  with minimal accuracy loss compared to FP32. One finding stands out: KD from a same-architecture teacher can fully ternarize ViT architecture’s most sensitive components like the patch embedding, layernorm and classifier head that prior work found extremely sensitive. Our compression pipeline’s primitives (like TernaryBitLinear, TernaryBitConv2d, TernaryLayerNorm) can also be used as standalone components in novel lightweight architectures. We show that the gap to FP32 scales inversely with model capacity [47]: 9.19 pp for DeiT-Tiny vs. 2.42 pp for DeiT-III-S<sup>384</sup>. In ImageNet-1K, FTerViT achieves 82.43% at 6.09 MB, surpassing previous ternary ViTs at higher compression, while 5.82 MB DeiT-III-S<sup>224</sup> deploys on a \$10 ESP32-S3.

**Limitations.** We evaluate DeiT-Tiny and DeiT-Small. Scaling to larger models is straightforward but orthogonal to our MCU focus. The C inference kernel uses basic bit-unpacking without optimization. The two-stage pipeline (training + fine-tuning) could potentially be unified into a single pass.

**Reproducibility.** All models were trained on a server equipped with 8 NVIDIA L40S GPUs between 1 and 2 days. Pretrained models and the codebase are available at <https://huggingface.co/szymonrucinski/FTerViT> and <https://github.com/szymonrucinski/FTerViT>.

## Acknowledgments and Disclosure of Funding

This research is supported by the Swiss National Foundation (219943) and SwissChips, a national initiative led by ETH Zürich, EPFL, and CSEM with funding from the State Secretariat for Education, Research and Innovation (SERI) to strengthen Switzerland’s semiconductor and IC-design ecosystem.

## References

- [1] Alexey Dosovitskiy et al. An image is worth 16x16 words: Transformers for image recognition at scale. *arXiv preprint arXiv:2010.11929*, 2020.
- [2] Hugo Touvron et al. Training data-efficient image transformers & distillation through attention. *ICML*, 2021.
- [3] Hugo Touvron, Matthieu Cord, and Hervé Jégou. Deit iii: Revenge of the vit. *ECCV*, 2022.
- [4] Pietro Bonazzi, Thomas Rüegg, Sizhen Bian, Yawei Li, and Michele Magno. Tinytracker: Ultra-fast and ultra-low-power edge vision for in-sensor gaze estimation. In *IEEE Sensors*, 2023.
- [5] Zhengqing Yuan et al. Vit-1.58b: Mobile vision transformers in the 1-bit era. *arXiv preprint arXiv:2406.18051*, 2024.
- [6] Sheng Xu, Yanjing Li, Teli Ma, Bohan Zeng, Baochang Zhang, Peng Gao, and Jinhu Lu. Tervit: An efficient ternary vision transformer. *arXiv preprint arXiv:2201.08050*, 2022.
- [7] Mikolaj Walczak, Uttej Kallakuri, Edward Humes, Xiaomin Lin, and Tinoosh Mohsenin. Bitmedvit: Ternary-quantized vision transformer for medical ai assistants on the edge. *ICCAD*, 2025.
- [8] Shu-Hao Zhang, Yue-Lu Gong, Kun-Peng Ning, Hao-Yang He, Yu-Jie Yuan, Jin-Dong Wang, and Shao-Qun Zhang. TernaryCLIP: Efficiently compressing vision-language models with ternary weights and distilled knowledge. *arXiv preprint arXiv:2510.21879*, 2025.
- [9] Yefei He et al. Bivit: Extremely compressed binary vision transformers. *ICCV*, 2023.
- [10] Yanjing Li et al. Bi-vit: Pushing the limit of vision transformer quantization. *AAAI*, 2024.
- [11] Phuoc-Hoan Charles Le and Xinlin Li. BinaryViT: Pushing binary vision transformers towards convolutional models. *CVPR Workshops*, 2023.
- [12] Junrui Xiao, Zhikai Li, Lianwei Yang, and Qingyi Gu. BinaryViT: Towards efficient and accurate binary vision transformers. *IEEE Transactions on Circuits and Systems for Video Technology*, 2025.
- [13] Yanjing Li et al. Q-vit: Accurate and fully quantized low-bit vision transformer. *NeurIPS*, 2022.
- [14] Shih-Yang Liu, Zechun Liu, and Kwang-Ting Cheng. Oscillation-free quantization for low-bit vision transformers. *ICML*, 2023.
- [15] Xijie Huang, Zhiqiang Shen, Pingcheng Dong, and Tim Kwang-Ting Cheng. Quantization variation: A new perspective on training transformers with low-bit precision. *TMLR*, 2024.
- [16] Matthieu Courbariaux, Itay Hubara, Daniel Soudry, Ran El-Yaniv, and Yoshua Bengio. Binarized neural networks: Training deep neural networks with weights and activations constrained to +1 or -1. *arXiv preprint arXiv:1602.02830*, 2016.
- [17] Shuchang Zhou, Yuxin Wu, Zekun Ni, Xinyu Zhou, He Wen, and Yuheng Zou. Dorefa-net: Training low bitwidth convolutional neural networks with low bitwidth gradients. *arXiv preprint arXiv:1606.06160*, 2016.
- [18] Zhen Dong, Zhewei Yao, Amir Gholami, Michael W. Mahoney, and Kurt Keutzer. Hawq: Hessian aware quantization of neural networks with mixed-precision. *ICCV*, 2019.
- [19] Zhenhua Liu, Yunhe Wang, Kai Han, Wei Zhang, Siwei Ma, and Wen Gao. Post-training quantization for vision transformer. *NeurIPS*, 2021.
- [20] Zhihang Yuan et al. Ptq4vit: Post-training quantization for vision transformers with twin uniform quantization. *ECCV*, 2022.
- [21] Yang Lin, Tianyu Zhang, Peiqin Sun, Zheng Li, and Shuchang Zhou. Fq-vit: Post-training quantization for fully quantized vision transformer. *IJCAI*, 2022.

- [22] Zhikai Li, Junrui Xiao, Lianwei Yang, and Qingyi Gu. Repq-vit: Scale reparameterization for post-training quantization of vision transformers. *ICCV*, 2023.
- [23] Lianwei Yang, Haisong Gong, and Qingyi Gu. DopQ-ViT: Towards distribution-friendly and outlier-aware post-training quantization for vision transformers. *TMLR*, 2024.
- [24] Navin Ranjan and Andreas Savakis. LRP-QViT: Mixed-precision vision transformer quantization via layer-wise relevance propagation. *TMLR*, 2024.
- [25] Yu-Shan Tai and An-Yeu Wu. AMP-ViT: Optimizing vision transformer efficiency with adaptive mixed-precision post-training quantization. *WACV*, 2025.
- [26] Pavlo Molchanov, Arun Mallya, Stephen Tyree, Iuri Frosio, and Jan Kautz. Importance estimation for neural network pruning. *CVPR*, 2019.
- [27] Shuming Ma, Hongyu Wang, Lingxiao Ma, Lei Wang, Wenhui Wang, Shaohan Huang, Li Dong, Ruiping Wang, Jilong Xue, and Furu Wei. The era of 1-bit llms: All large language models are in 1.58 bits. *arXiv preprint arXiv:2402.17764*, 2024.
- [28] Fengfu Li, Bo Zhang, and Bin Liu. Ternary weight networks. *arXiv preprint arXiv:1605.04711*, 2016.
- [29] Yoshua Bengio, Nicholas Léonard, and Aaron Courville. Estimating or propagating gradients through stochastic neurons for conditional computation. *arXiv preprint arXiv:1308.3432*, 2013.
- [30] Markus Nagel, Mart van Baalen, Tijmen Blankevoort, and Max Welling. Data-free quantization through weight equalization and bias correction. *ICCV*, 2019.
- [31] Raghuraman Krishnamoorthi. Quantizing deep convolutional networks for efficient inference: A whitepaper. *arXiv preprint arXiv:1806.08342*, 2018.
- [32] Zechun Liu, Zhiqiang Shen, Marios Savvides, and Kwang-Ting Cheng. ReActNet: Towards precise binary neural network with generalized activation functions. *ECCV*, 2020.
- [33] Minsoo Kim, Sihwa Lee, Sukjin Hong, Du-Seong Chang, and Jungwook Choi. Understanding and improving knowledge distillation for quantization aware training of large transformer encoders. *EMNLP*, 2022.
- [34] Navin Ranjan and Andreas Savakis. Vision transformer quantization with multi-step knowledge distillation. *arXiv preprint arXiv:2406.14004*, 2024.
- [35] Kaiqi Zhao and Ming Zhao. Self-supervised quantization-aware knowledge distillation. *AIS-TATS*, 2024.
- [36] Sharath Turuvekere Sreenivas, Saurav Muralidharan, Raviraj Joshi, Marcin Chochowski, Ameya Sunil Mahabaleshwarkar, Gerald Shen, Jiaqi Zeng, Zijia Chen, Yoshi Suhara, Shizhe Diao, Chenhan Yu, Wei-Chun Chen, Hayley Ross, Oluwatobi Olabiyi, Ashwath Aithal, Oleksii Kuchaiev, Daniel Korzekwa, Pavlo Molchanov, Mostofa Patwary, Mohammad Shoeybi, Jan Kautz, and Bryan Catanzaro. LLM pruning and distillation in practice: The Minitron approach. *arXiv preprint arXiv:2408.11796*, 2024.
- [37] Meng Xin, Sweta Priyadarshi, Jingyu Xin, Bilal Kartal, Aditya Vavre, Asma Kuriparambil Thekkumpate, Zijia Chen, Ameya Sunil Mahabaleshwarkar, Ido Shahaf, Akhiad Bercovich, et al. Quantization-aware distillation for nvfp4 inference accuracy recovery. *arXiv preprint arXiv:2601.20088*, 2026.
- [38] Kan Wu, Jinnian Zhang, Houwen Peng, Mengchen Liu, Bin Xiao, Jianlong Fu, and Lu Yuan. TinyViT: Fast pretraining distillation for small vision transformers. *ECCV*, 2022.
- [39] Seungwoo Son, Jegwang Ryu, Namhoon Lee, and Jaeho Lee. The role of masking for efficient supervised knowledge distillation of vision transformers. *arXiv preprint arXiv:2302.10494*, 2023.
- [40] Shangquan Sun, Wenqi Ren, Jingzhi Li, Rui Wang, and Xiaochun Cao. Logit standardization in knowledge distillation. *CVPR*, 2024.

- [41] Ilya Loshchilov and Frank Hutter. Decoupled weight decay regularization. *ICLR*, 2019.
- [42] Steven K. Esser, Jeffrey L. McKinstry, Deepika Bablani, Rathinakumar Appuswamy, and Dharmendra S. Modha. Learned step size quantization. *ICLR*, 2020.
- [43] Samira Abnar and Willem Zuidema. Quantifying attention flow in transformers. *Proc. ACL*, 2020.
- [44] Yinan Liang, Ziwei Wang, Xiuwei Xu, Yansong Tang, Jie Zhou, and Jiwen Lu. Mcuformer: Deploying vision transformers on microcontrollers with limited memory. *arXiv preprint arXiv:2310.16898*, 2023.
- [45] Jianlei Yang, Jiacheng Liao, Fanding Lei, Meichen Liu, Lingkun Long, Junyi Chen, Han Wan, Bei Yu, and Weisheng Zhao. Tinyformer: Efficient transformer design and deployment on tiny devices. *arXiv preprint arXiv:2311.01759*, 2023.
- [46] Christophe El Zeinaty, Wassim Hamidouche, Glenn Herrou, Daniel Ménard, and Mérouane Debbah. Can llms revolutionize the design of explainable and efficient tinymodels? *IJCNN*, 2025.
- [47] Ouyang Xu, Tao Ge, Thomas Hartvigsen, Zhisong Zhang, Haitao Mi, and Dong Yu. Low-bit quantization favors undertrained LLMs: Scaling laws for quantized LLMs with 100T training tokens. *arXiv preprint arXiv:2411.17691*, 2024.
- [48] Ali Hassani, Steven Walton, Nikhil Shah, Abulikemu Abuduweili, Jiachen Li, and Humphrey Shi. Escaping the big data paradigm with compact transformers. *arXiv preprint arXiv:2104.05704*, 2021.
- [49] Shashank Nag, Alan T. L. Bacellar, Zachary Susskind, Anshul Jha, Logan Liberty, Aman Sivakumar, Eugene B. John, Karthik Kailas, Paulo M. Lima, Neeraja Yadwadkar, Felipe M. G. França, and Lizy K. John. Ll-vit: Edge deployable vision transformers with look up table neurons. *FPT*, 2025.
- [50] Zhikai Li and Qingyi Gu. I-vit: Integer-only quantization for efficient vision transformer inference. *ICCV*, 2023.
- [51] Mark Sandler, Andrew Howard, Menglong Zhu, Andrey Zhmoginov, and Liang-Chieh Chen. Mobilenetv2: Inverted residuals and linear bottlenecks. *CVPR*, 2018.

## A Experiments Appendix

### A.1 Benchmark Results on CIFAR-10 and CIFAR-100

As shown in Table 6, our ternary model achieves 97.43% top-1 accuracy on CIFAR-10 and 86.01% on CIFAR-100. These results are within 0.09% and 0.53% of the full-precision DeiT-Tiny baseline while reducing the model size by  $15\times$  (from 22.9 MB to 1.53 MB). FTerDeiT-Tiny substantially outperforms all compared INT8 and ternary models, including recent low-bitwidth ViTs and CNNs.

Table 6: Prior work comparison on CIFAR-10 and CIFAR-100.

Method	Params (M)	Size (MB)	Top-1 Accuracy	
			CIFAR-10	CIFAR-100
<b>Full-precision</b>				
DeiT-Tiny (pretrained) [2]	5.5	22.9	97.52%	86.54%
CCT-7/3x1 [48]	3.76	15	96.5%	—
<b>INT8 quantized</b>				
TinyFormer-300K [45]	0.73	0.91	96.10%	—
LL-ViT [49]	2.5	1.93	95.5%	78.8%
I-ViT-T [50]	5.3	5.3	95.4%	79.2%
MobileNetV2 [51]	2.2	2.13	94.61%	—
LMaNet-Elite [46]	<1	<1	—	74.50%
<b>Ternary</b>				
ViT-1.58b [5]	307	57	72.3%	—
<b>FTerDeiT-Tiny (Ours)</b>	<b>5.5</b>	<b>1.53</b>	<b>97.43%</b>	<b>86.01%</b>

## B On-Device Deployment and Profiling

### B.1 Latency and Memory Results

Table 7: On-device inference profile for DeiT-III-S<sup>224</sup> on ESP32-S3-EYE (dual Xtensa LX7 @ 240 MHz, 8 MB octal PSRAM, SIMD path)

Component	Time/block	12 blocks	% total
LayerNorm (pre + post)	38 ms	456 ms	2.2%
QKV projection (fused)	146 ms	1,752 ms	8.3%
Attention (Q@K <sup>T</sup> +softmax+V)	551 ms	6,612 ms	31.4%
Output projection	70 ms	840 ms	4.0%
FFN (fc1 + fc2)	549 ms	6,588 ms	31.3%
<b>Total (12 blocks)</b>		<b>16,248 ms</b>	77.1%
Patch embed + head + other		4,814 ms	22.9%
<b>End-to-end latency</b>		<b>21,062 ms</b>	100%
Throughput		0.0475 inf/s	—
<i>Memory &amp; storage</i>			
Flash (weights, ternary)		5.81 MB	—
Flash (firmware, code+rodota)		0.50 MB	—
Flash partition used / free		6.30 / 8.00 MB	79% used
Peak PSRAM (HWM, measured)		<b>2.83 MB</b>	—
of which scratch		1.89 MB	—
of which input image		0.57 MB	—
of which camera/LCD		≈ 0.37 MB	—
PSRAM heap available		7.35 MB	—
Internal SRAM min-free		93.9 KB	—
<i>Compression vs FP32</i>			
FP32 .pth reference		88.3 MB	—
Ternary flash footprint		5.81 MB	—
ImageNet-1K top-1 accuracy		79.64%	—